AMS 2024 Annual Meeting 28 January – 1 February, 2024

V3

The Volcanic Eruption Observed by the Satellite Microwave Measurements and the MiRS Temperature Retrieval
The Hunga Tonga-Hunga Ha'apai Volcanic Eruption case

Yong-Keun Lee[1], Neil Hindley[2], Christopher Grassotti[1] , Quanhua Liu[3]

1. University of Maryland, Cooperative Institute for Satellite Earth System Studies and NOAA/NESDIS/STAR (yong-keun.lee@noaa.gov) 2. University of Bath, UK 3. NOAA/NESDIS/STAR

Abstract

The strongest volcanic eruption since the 19th century occurred on January 15, 2022 at Hunga Tonga-Hunga Ha'apai, generating unprecedented atmospheric waves not seen before in observations. We used satellite microwave observations from (1) Advanced Technology Microwave Sounder (ATMS) on board the National Oceanic and Atmospheric Administration (NOAA)-20 and the Suomi-National Polar-orbiting Partnership (SNPP) and (2) Advanced Microwave Sounding Unit (AMSU)-A on board Meteorological operational satellite (MetOp)-B/MetOp-C to study these waves in the stratosphere immediately after the eruption. The NOAA Microwave Integrated Retrieval System (MiRS) was applied to these microwave observations to produce atmospheric temperature profiles. The atmospheric Lamb wave and fast-traveling gravity waves are clearly revealed in both the brightness temperatures and the MiRS retrieved temperatures, revealing their vertical phase structures. This study is the first attempt to perform a detailed analysis of the stratospheric impact of the Tonga eruption on operational satellite microwave observations and the corresponding MiRS retrievals.

Data and Methods

Initial volcanic eruption: 4:28 UTC January 15, 2022 20.536 °S 175.382 °W
NOAA-20/SNPP ATMS: 22 microwave channels (01/15/2022)
Metop-B/Metop-C AMSU-A & MHS: 20 microwave channels (01/15/2022)
MiRS: The NOAA Microwave Integrated Retrieval System
: atmospheric temperature, water vapor, hydrometeor profiles for 100 layers
: surface variables including surface temperature and surface emissivity

The difference calculation (local 3x3 FOV average minus the polynomial curve fit) was applied for each pressure layer of atmospheric temperature profiles and for each channel of ATMS and AMSU-A brightness temperatures to determine the perturbation.
The formula for 2-D polynomial curve fit is given below.

$$\begin{aligned} \text{fitresult}(x,y) = {} & p00 + p10*x + p01*y + p20*x^2 + p11*x*y \\ & + p02*y^2 + p30*x^3 + p21*x^2*y + p12*x*y^2 + p03*y^3 \\ & + p40*x^4 + p31*x^3*y + p22*x^2*y^2 + p13*x*y^3 \\ & + p04*y^4 + p50*x^5 + p41*x^4*y + p32*x^3*y^2 \\ & + p23*x^2*y^3 + p14*x*y^4 + p05*y^5 \end{aligned}$$

x represents longitude, y latitude, pij polynomial coefficients, i and j are integer exponents for x and y, respectively.

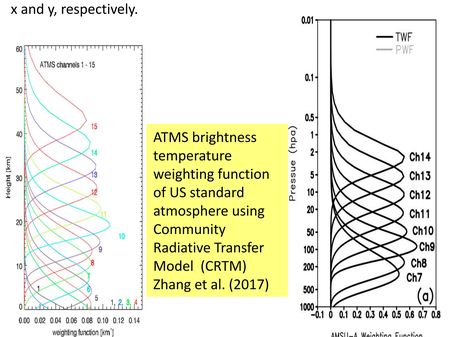

ATMS brightness temperature weighting function of US standard atmosphere using Community Radiative Transfer Model (CRTM) Zhang et al. (2017)

AMSU-A brightness temperature weighting function of US standard atmosphere using Community Radiative Transfer Model (CRTM) Zou and Qian. (2016)

Acknowledgement and Disclaimer

This work is supported by NOAA under Grant NA19NES4320002 to the Cooperative Institute for Satellite and Earth System Studies (CISESS) at the University of Maryland/Earth System Science Interdisciplinary Center (ESSIC). The views, opinions, and findings contained in this presentation are those of the authors and should not be construed as an official NOAA or U.S. Government position, policy, or decision.

BT signal from the upper stratosphere

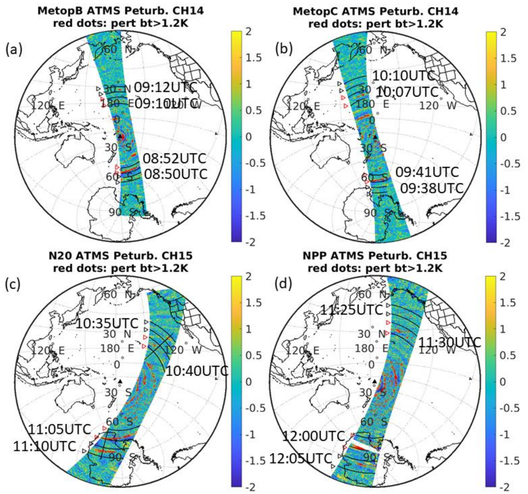

Figure 1. The local perturbations in observed microwave brightness temperatures from an ascending orbit of (a) MetOp-B AMSU-A channel 14, (b) MetOp-C AMSU-A channel 14, a descending orbit of (c) NOAA-20 ATMS channel 15, and (d) SNPP ATMS channel 15 on January 15, 2022. The black triangle at the center for each panel is the Tonga volcano location. The outermost black-curved lines from the Tonga volcano location correspond to a phase speed of 330 m/s assuming that the perturbation has been generated at the time and location of initial volcanic eruption. From the 2nd outermost black-curved lines to the innermost lines, the phase speeds are 300, 270, and 230 m/s, respectively. The time information in each panel indicates the approximate observation time for the Lamb wave (between 300 m/s and 330 m/s indicated by black right-pointing triangles) and for the lead gravity wave (between 230 m/s and 270 m/s indicated by red right-pointing triangles). Red dots indicate the pixels where the brightness temperature perturbation is larger than 1.2 K. Two black-straight lines in (c) are used in Fig. 2(a) to show perturbations following each line.

BT signal for each frequency

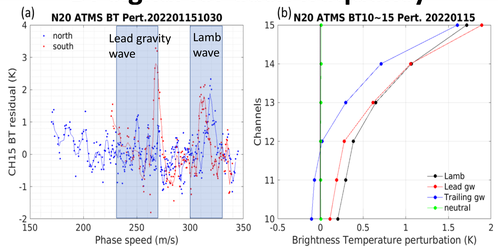

Figure 2. (a) NOAA-20 ATMS brightness temperature (channel 15) perturbations following two straight-black lines that extend from the Tonga eruption location in Fig. 1(c). Perturbation data are shown for the northern and southern lines using blue and red symbols, respectively. The overlapped lines are 5 pixel moving average for each. Light-blue shaded areas correspond to equal phase speed lines in Fig.1(c) for the Lamb wave and the first lead gravity wave, respectively. (b) NOAA-20 ATMS brightness temperature perturbation by channels between 10 and 15 for each wave on January 15, 2022. The perturbation curves are based on a selection of pixels (FOVs) in the vicinity of the wave crests. The curve corresponding to "neutral" indicates the FOVs not affected by the volcanic eruption located at distances beyond the fastest moving Lamb wave. The numbers of pixels used in these figures are 362, 597, 696, and 27376 for the Lamb wave, the lead gravity wave, the trailing waves, and non-atmospheric wave (neutral) area, respectively.

Atmospheric Temperature in the upper stratosphere

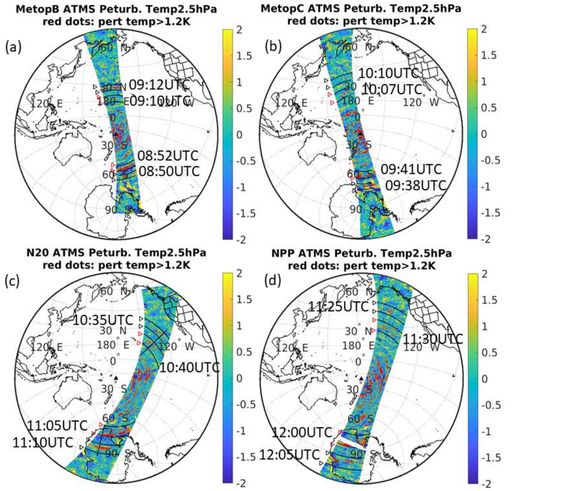

Figure 3. The local perturbations of the MiRS retrieved atmospheric temperature from (a) an ascending orbit of (a) MetOp-B AMSU-A, (b) MetOp-C AMSU-A, a descending orbit of (c) NOAA-20 ATMS, (d) SNPP ATMS at 2.5 hPa on January 15, 2022. The black-curved lines and the time information in each panel are the same as Fig. 1. Red dots indicate the pixels where atmospheric temperature perturbation is larger than 1.2 K. Two black-straight lines in (c) are used in Fig. 4(a) to show perturbations following each line.

Vertical structure of Atmospheric Temperature

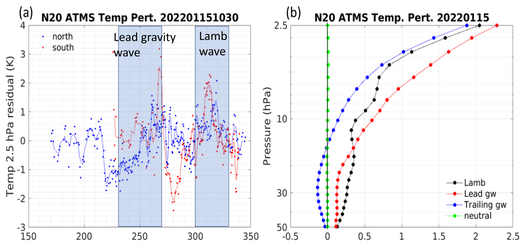

Figure 4. Same as Fig. 2 except for MiRS NOAA-20 ATMS retrieved atmospheric temperature perturbation (a) at 2.5 hPa following two straight-black lines in Fig. 3(c) and (b) vertical structure between 2.5 and 50 hPa.

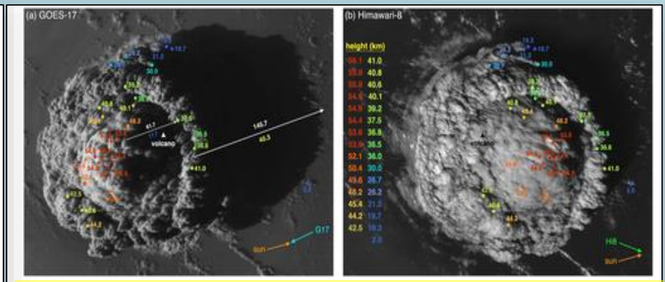

Figure 5. Image of the plume on 15 January 2022 at 04:30Z from (a) GOES-17 and (b) Himawari-8. Colored dots mark manual stereo height estimates (in km), and the white/black triangles show the volcano's location. The white arrows in panel (a) depict the shadow of a plume edge feature and a dome feature, with the shadow length and the derived height given above/below the arrow. Arrows in the lower right of each panel indicate the sun-to-pixel and satellite-to-pixel azimuths. Carr et al. (2022)

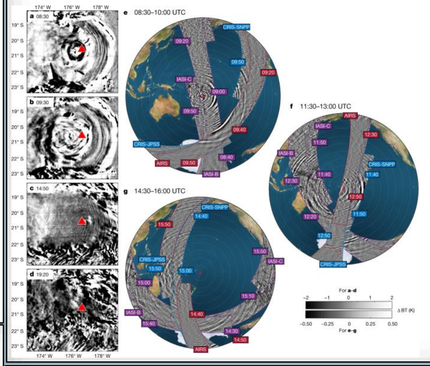

Figure 6. **Post-eruption gravity wave activity**: (a-d) in and around the volcanic plume as observed by GOES and (e-g) over the entire Pacific basin as observed by AIRS, CrIS and IASI. For (e-g) coloured labels indicate individual satellite overpass times for context, with AIRS labelled in red, CrIS in blue and IASI in purple. Note that the colour scales in panels (a) and (b) saturate significantly, and values extend to ±8K.Wright et al. (2022)

Summary

- Microwave observations from multiple satellites capture stratospheric waves from the Tonga eruption, including Lamb and gravity waves.
- MiRS atmospheric temperature retrievals also resolve wave perturbations in the stratosphere after the eruption.
- The Lamb wave and the lead gravity wave show no apparent phase change with height, whereas the trailing gravity waves do.

References

Carr, J. L., A. Horvath, D. L. Wu, and M. D. Friberg (2022). Stereo plume height and motion retrievals for the record setting Hunga Tonga-Hunga Ha'apai eruption of 15 January 2022, Geophysical Research Letters, 49, e2022GL098031, https://doi.org/10.1029/2022GL098131.

Lee, Y.-K., Hindley, N., Grassotti, C., & Liu, Q. (2023). The Hunga Tonga-Hunga Ha'apai volcanic eruption as seen in satellite microwave observations and MiRS temperature retrievals. Geophysical Research Letters, 50, e2023GL106439.

Wright, C. J. et al. (2022). Surface-to-space atmospheric waves from Hunga Tonga-Hunga Ha'apai eruption. Nature https://doi.org/10.1038/s41586-022-05012-5.

Zhang, K., L. Zhou, M. Goldberg, X. Liu, W. Wolf, C. Tan, and Q. Liu (2017). A Methodology to Adjust ATMS Observations for Limb Effect and Its Applications, Journal of Geophysical Research: Atmospheres, 122, 11347-11356, https://doi.org/10.1002/2017JD026820.

Zou, C.-Z, and H. Qian (2016). Stratospheric temperature climate data record from merged SSU and AMSU-A observations, Journal of Atmospheric and Oceanic Technology, 33(9), 1967-1984, https://doi.org/10.1175/JTECH-D-16-0018.1.